Development 129, 143-154 (2002)
Printed in Great Britain © The Company of Biologists Limited 2002
DEV5977



# Eyes closed, a *Drosophila* p47 homolog, is essential for photoreceptor morphogenesis

**Tzu-Kang Sang and Donald F. Ready***

Department of Biological Sciences, Purdue University, West Lafayette, IN 47907, USA
*Author for correspondence (e-mail: dready@bilbo.bio.purdue.edu)

*Accepted 2 October 2001*

## SUMMARY

**Starting with a mutation impacting photoreceptor morphogenesis, we identify here a *Drosophila* gene, *eyes closed* (*eyc*), as a fly homolog of p47, a protein co-factor of the p97 ATPase implicated in membrane fusion. Temporal misexpression of Eyc during rhabdomere extension early in pupal life results in inappropriate retention of normally transient adhesions between developing rhabdomeres. Later Eyc misexpression results in endoplasmic reticulum proliferation and inhibits rhodopsin transport to the developing photosensitive membrane. Loss of Eyc function results in a lethal failure of nuclear envelope assembly in early zygotic divisions. Phenotypes resulting from *eyc* mutations provide the first in vivo evidence for a role for p47 in membrane biogenesis.**

Key words: *Drosophila*, Photoreceptor, Rhabdomere morphogenesis, p47, p97, Membrane fusion, Nuclear envelope

Movies available on-line

## INTRODUCTION

Molecular change is a hallmark of membrane differentiation; developing cells deploy distinct protein assemblies in and around the plasma membrane appropriate for the task at hand. Common tasks during development include reorganization of adhesive contacts between cells and the establishment of well-ordered plasma membrane subdomains. Directed membrane traffic is fundamental to such reorganization, but much remains to be learned of how it contributes.

Starting with the identification of a *Drosophila* eye mutant, *eyes closed* (*eyc*$^{1}$), in which fragmented rhabdomeres engage in inappropriate contact, we have identified a homolog of mammalian p47, a protein associated with membrane fusion. Temporal misexpression of Eyc in developing pupal eyes results in inappropriate retention of adhesive contacts that mediate rhabdomere extension, an early determinant of photoreceptor morphogenesis, and failure to subdivide photoreceptor apical membranes into the normal center-surround domains of the photosensitive rhabdomere and its surrounding stalk domain. Loss of *eyc* results in lethal failure of nuclear envelope assembly in early zygotic divisions, a novel role for p47 in cell cycle regulated membrane fusion in higher eukaryotic cells. Phenotypes resulting from *eyc* mutations provide the first in vivo evidence for a role for p47 in membrane biogenesis and development.

Membrane fusion is fundamental to virtually all aspects of cell physiology, including vesicle-mediated transport through the secretory pathway and the postmitotic reconstitution of Golgi, endoplasmic reticulum (ER) and nuclear membranes from mitotic vesicles (Guo et al., 2000; Mellman and Warren, 2000; Rothman and Warren, 1994). Substantial evidence suggests fusion is mediated by SNARE (soluble N-ethylmaleimide-sensitive factor attachment protein receptor) integral membrane proteins, assisted by a host of additional cytoplasmic proteins, including two ATPases, NSF (N-ethylmaleimide-sensitive factor) (Block et al., 1988) and p97 (Acharya et al., 1995; Latterich et al., 1995; Rabouille et al., 1995). These ATPases disassemble unproductive *cis*-SNARE complexes, priming them for fusion by making SNAREs available to engage in *trans* with cognate SNAREs of target membranes and thereby promoting another round of fusion (Mayer et al., 1996; Rabouille et al., 1995). Although exceptions exist, NSF is typically targeted by α-SNAP (soluble NSF attachment protein α) to SNARE complexes that result from heterotypic membrane fusion, while p97 is targeted by p47 to complexes resulting from homotypic membrane fusion (Edwardson, 1998; Mellman, 1995).

p47 was first found complexed with p97 in an in vitro Golgi reassembly assay (Kondo et al., 1997). Loss of p47 results in the failure to reassemble Golgi stacks after their vesiculation during mitosis. Stoichiometry is a crucial determinant of p47/p97 activity; ratios above or below optimal decrease Golgi reassembly (Meyer et al., 1998). Co-operation between NSF and p97 pathways is suggested by the competition of α-SNAP and p47 for a common syntaxin-5 SNARE complex (Rabouille et al., 1998). Both pathways are required to rebuild Golgi cisternae from mitotic Golgi fragments in vitro; alone, each promotes vesicle fusion leading to morphologically distinct cisternae (Acharya et al., 1995; Rabouille et al., 1995). Fusion

of ER membranes from yeast mutant for the p97 homolog, *CDC48*, is inhibited in an in vitro assay (Latterich et al., 1995). Similarly, a rat liver microsome fusion assay also demonstrates a requirement for p97 in ER assembly (Roy et al., 2000). In addition to its role in membrane fusion, p97 also participates in other activities, including ubiquitin-dependent protein degradation, nuclear transport pathways and DNA unwinding (Meyer et al., 2000; Yamada et al., 2000). p97 activity is directed to different cellular pathways by the regulation of its co-factors. A role for p47 has not been described in development and morphogenesis.

Photoreceptor morphogenesis demands a high level of performance by mechanisms mediating directed membrane traffic. Rhabdomeres, like their vertebrate counterparts, the outer segments of rod and cone photoreceptors, are enormously amplified central subdomains of the photoreceptor apical membrane. Rhabdomere growth during pupal life is driven by delivery of copious photosensitive membrane to the developing rhabdomere. Defects in membrane traffic yield rhabdomere defects, which are plain against the precise, stereotyped and sizeable rhabdomeres of normal flies; *Drosophila* photoreceptor morphogenesis is a sensitive assay of membrane differentiation.

## MATERIALS AND METHODS

### Fly strains

The *fliA*$^{4}$ strain was provided by E. Fyrberg (Johns Hopkins University). In addition to the mutation in *fliA* that encodes the *Drosophila* α-Actinin, it contains a second mutation affecting eye development. The fly stocks *w; Sco/SM1; TM2/MKRS*, *Sp*$^{1}$*J*$^{1}$*L*$^{2}$*Pin*$^{1}$*/SM5*, *Df(2R)Px2*, *b*$^{1}$ *Adh* ch* l(2)**/CyO; ry*$^{506,}$ *Sp/CyO; ry*$^{506}$ *Sb* P{ry$^{+7.2}$=Δ2-3}/*TM6*, *cn*$^{1}$P{ry$^{+7.2}$=PZ}l(2) 04012/*CyO; ry*$^{506}$ (P1363), P{ry$^{+7.2}$=neoFRT}42D and *y*$^{1}$*w**; P{ry$^{+7.2}$=neoFRT}42D P{y$^{+7.7}$ ry$^{+7.2}$=Car20y}44B P{w$^{+mc}$=GMR-hid}SS2 *l(2)CL-R*$^{1/}$*CyO*; P{w$^{+m}$*=GAL4-ey.H}SS5 P{w$^{+mc}$=UAS-FLP1.D}JD2 (*EGUF/hid*) were obtained from the Bloomington Stock Center.

### Genetics

Flies were raised on standard corn meal-agar media at 25°C. Fly crosses were carried out according to standard procedures. *eyc*$^{1}$ mutant was isolated from the *fliA*$^{4}$ strain by crossing *fliA*$^{4}$ fly with *w; Sco/SM1; TM2/MKRS*. Meiotic mapping of the *eyc* gene was carried out by crossing *eyc*$^{1}$ to the second chromosome dominant marker strain *Sp*$^{1}$*J*$^{1}$*L*$^{2}$*Pin*$^{1}$*/SM5*. Recombination frequency based on deep pseudopupil screening placed the *eyc* locus in the tip of 2R, very close to *Pin* (genetic location 2-107.3). Deficiency strains within the mapped region were collected and used to refine the location of *eyc*. One deficiency line, *Df(2R)Px2* (break points 60C5-D2), fails to complement *eyc*$^{1}$. We collected P-element insertion lines, which have been placed in the refined mapping region 60C5-60D2 and found *cn*$^{1}$P{ry$^{+7.2}$=PZ}l(2) 04012/*CyO; ry*$^{506}$ (P1363), which maps to 60D1-2 (generated by A. Spradling), failed to complement *eyc*$^{1}$; P1363/*Df(2R) Px2* flies display an *eyc*-like eye phenotype (Fig. 1D). In order to verify that P1363 is an *eyc* allele, we remobilized the P-element by crossing P1363 virgins to *Sp/CyO; ry*$^{506}$ *Sb P{ry*$^{+7.2}$*=Δ2-3}/TM6* males. Male progeny *cn*$^{1}$*P{ry*$^{+7.2}$*=PZ}l(2)04012/Sp; ry*$^{506}$*/ry*$^{506}$ *Sb P{ry*$^{+7.2}$*=Δ2-3}* were selected and crossed to *b*$^{1}$ *Adh* ch* l(2)**/CyO; ry*$^{506}$. *CyO* progeny with *ry*$^{-}$ eyes were single pair mated to *Sp/CyO; ry*$^{506}$. Sibling *CyO*, non-*Sp* progeny were crossed to produce lines homozygous for the P-element excision chromosome. We expected that precise excision lines should generate homozygous viable progeny, but we failed to recover any after screening 250 lines. This is probably due to a deletion we subsequently found in the original P1363 chromosome (see Results). We recombined P1363 onto a wild type background to eliminate this deletion and generated a P1363 homozygous viable line, *eyc*$^{P}$. We then repeated P-element remobilization. Precise excision of the P-element, determined by PCR assay, restored normal eye morphology. Additional *eyc* alleles generated by imprecise excision in *trans* with the original *eyc*$^{1}$ allele show rhabdomeres similar to *eyc*$^{1}$ homozygous.

To generate *eyc* loss-of-function alleles, the P-element of *eyc*$^{P}$ was remobilized; 27 out of 250 lines screened were homozygous lethal. *eyc*$^{l39}$, which removes the *eyc* ORF has an intact downstream gene was used as an *eyc* null allele.

To generate homozygous *eyc* null eyes, *eyc*$^{l39}$ was recombined onto the P{ry$^{+7.2}$=neoFRT}42D chromosome, and balanced over *CyO*. When crossed to *EGUF/hid* flies, flippase activity provided by the EGUF chromosome promotes somatic recombination, homozygosing *eyc*$^{l39}$ in the eye (Stowers and Schwarz, 1999). Eye clones were examined among non-*CyO* progeny.

### Molecular analysis

DNA flanking the P1363 insertion site was isolated by plasmid rescue. Briefly, genomic DNA of adult P1363 flies was isolated, digested using *Xba*I+*Nhe*I or *Hpa*I, religated and transformed into DH5α competent cells (Life Technologies) and selected for kanamycin resistant colonies. Genomic DNA flanking the P-element was recovered, restriction enzyme digested and used as hybridization probes to identify transcripts in wild type (Canton S) and *eyc*$^{1}$ flies. One genomic probe, P3, detected a high level of mRNA expression in *eyc*$^{1}$ mutants which was nearly absent in wild type at about 30% pupal development (p.d.). The P3 probe was used to screen a λt11 adult head cDNA library (provided by W. Pak; original library constructed by E. Buchner). Twelve clones were isolated and all contained a 1.1 kb DNA fragment. This 1.1 kb cDNA was sequenced on both strands.

For Northern hybridization, poly(A)$^{+}$mRNA from 0.5g mid-pupal stage flies was prepared by using PolyATract®System 1000 (Promega), fractionated in a 1.2% agarose/formaldehyde gel, and transferred to Hybond™-N+ positive charged nylon membrane (Amersham). Membranes were hybridized to $^{32}$P-labeled genomic DNA probes or cDNA probe according to the manufacturer's instructions.

### Germline transformation

A 1112 bp fragment that covers the *eyc* ORF was excised from an *Eco*RI digested cDNA clone and cloned into pUAST to construct pUAST-eyc. Germline transformation was performed according to standard procedures (Spradling and Rubin, 1982). Briefly, *w*$^{1118}$ embryos were injected with pUAST-eyc and helper plasmid Δ2-3. Transformants with *w*$^{+}$ eye color were mapped and homozygosed by crossing to the balancer *w; Sco/SM1; TM2/MKRS*.

### Electron microscopy and immunohistochemistry

Flies were prepared for transmission electron microscopy as described by Baumann and Walz (Baumann and Walz, 1989), with modifications. Fly eyes were dissected and fixed with aldehyde fixative (2% paraformaldehyde and 1.75% glutaraldehyde in 0.1 M sodium cacodylate, pH 7.4). Fixed eyes were then incubated in 1% tannic acid overnight followed by post-fixation in 0.1 M sodium cacodylate with 2% osmium tetroxide for 2 hours. After washing, eyes were incubated in 2% uranyl acetate overnight and dehydrated through an ethanol series. The samples were mounted and sectioned as described by Tomlinson and Ready (Tomlinson and Ready, 1987). Samples were observed using a Philips 300 electron microscope.

Phalloidin and immunostaining were performed with whole-mount preparation as previously described (Chang and Ready, 2000), with modifications. For immunohistochemistry, staged eyes were dissected

and fixed in 4% formaldehyde in phosphate-buffered saline (PBS) for 1 hour. The brain was removed approximately 30 minutes into fixation. Fixed eyes were then given three 10 minute washes in PBST (PBS plus 0.3% Triton X-100). Washed eyes were incubated in primary antibody: anti-Armadillo (1:50), anti-Rh1 (1:50, both obtained from Hybridoma Bank, the University of Iowa), anti-Crumbs (1:300, generous gift from U. Tepass) (Tepass, 1996), or in 2 μg/ml rhodamine-conjugated phalloidin (Sigma) in PBST plus 5% goat serum overnight at 4°C. For detecting DE-Cadherin, staged eyes were fixed in the fixative contains 1 mM $CaCl_2$, the eyes were stained in 1:20 diluted anti-DE-cadherin antibody (a generous gift from T. Uemura) (Uemura et al., 1996). Eyes were given three 10 minutes washes in PBST and were then incubated for 4 hours at room temperature in secondary antibody. After incubation, eyes were given three 10 minutes PBST washes and mounted (0.25% n-propyl gallate, 50% glycerol in PBS, pH 8.6).

For embryo immunohistochemistry, staged embryos were collected from juice plates. Fixation and hand-devitellinization embryo followed protocols of White (White, 1998). Anti-Lamin antibody was a generous gift from P. Fisher (Smith and Fisher, 1989; Stuurman et al., 1995). YOYO-1 was purchased from Molecular Probes (Eugene) and used according to the manufacturer's instructions.

Samples were examined using a BioRad MRC-1024 confocal microscope.

### Antibody production and western blot

Rabbit anti-Eyc antiserum, raised against the bacterial expressed histidine-tagged full length Eyc, was made by Bethyl Laboratories. In brief, *eyc* cDNA was subcloned into pTrcHisC vector (Invitrogen) and the junction sites were sequencing verified to ensure the construct was in frame. His-Eyc fusion protein was expressed in the bacterial strain JM109 and the fusion protein was purified by TALON resin (Clontech). A expected 45 kDa band was excised from SDS-PAGE and electroelution purified as immunogen.

Proteins were resolved by SDS-PAGE, and then transfer to nitrocellulose membrane. Western blots were blocked with 5% nonfat dry milk in TBST (20 mM Tris-HCl pH 7.6, 137 mM NaCl and 0.5% Tween 20) for 2 hours at room temperature and then probed with anti-Eyc antiserum (1:2000) in blocking reagent overnight at 4°C. Following incubation with peroxidase-conjugated goat anti-rabbit IgG (Vector), blots were detected using SuperSignal chemiluminescent substrates (Pierce).

### Antibody inhibition

Stage 2-3 embryos were collected and prepared for microinjection according to standard procedure. Approximately 5/100 egg volume of serum (~0.6 g/ml protein) was injected into the posterior end of the embryo. After 1 hour's recovery, injected embryos were prepared for immunohistochemistry.

## RESULTS

### Genesis of rhabdomere trapezoids

The trapezoid of adult rhabdomeres (Fig. 1A) has its origin early in pupal life with the establishment of a stereotyped set of contacts between photoreceptor apical faces, the future rhabdomeres. While maintaining the zonula adherens (z.a.) junctions formed during pattern formation, inpocketing of photoreceptor apices into the retinal epithelium by closure of the lens-secreting cone cells 'above' them, brings photoreceptors 'face-to-face' in a trapped apical cavity that is the precursor of the inter-rhabdomeral space (IRS) (see Movie at http://dev.biologists.org/supplemental/). Contacts between photoreceptors R2, R4 and R7 occlude R3 from the center of the ommatidium, displacing its apical membrane to the future 'point' of the trapezoid. Between 37% p.d. and 55% p.d., photoreceptor apical surface amplification extends these contacts to the retinal floor, along a 'core' of partitions at the center of the ommatidium; photoreceptor apices meet in a manner resembling the sectors of an orange (Fig. 1E,G). During extension, the previously undifferentiated apical membrane is reorganized in center-surround domains dedicated to future development of rhabdomere and stalk membrane. By 55% p.d., face-to-face contacts between photoreceptors are relinquished, opening the IRS (Fig. 1G) (Longley and Ready, 1995).

In order to further characterize contacts between photoreceptor apical faces, we stained developing eyes between 37% p.d. and 55% p.d. using phalloidin and antibodies to the apical membrane protein, Crumbs (Crb) as well as antibodies against Armadillo (Arm, *Drosophila* β-Catenin) and anti-*Drosophila* E-cadherin (DE-Cad), proteins associated with adhesive cell-cell contacts that are typically localized to z.a. junctions. Confocal images of wild type 37% p.d. eyes show Crb, Arm and DE-Cad across the entire apical membrane, in addition to strong staining in z.a. junctions (Fig. 2A) (wild type 37% p.d.). By 50% p.d., the stage when apical face contacts are released, Arm and DE-Cad have retreated from the apical surface and stain only the z.a junctions. These results suggest that the 'unsticking' of R cell apical faces by 50% p.d. may be due to reorganization of Arm and DE-Cad in the R cell apical membrane.

Distinct programs of membrane reorganization mark photoreceptor differentiation. Between 55% and 70% p.d., the apical membrane protein Crb (Tepass, 1996) is relocalized from the entire surface (Fig. 2A) to the stalk (U. Tepass and D. Ready, unpublished). This redistribution occurs in *eyc* mutants.

### Isolation of *eyc*$^{1}$ and phenotypic characterization

We have found previously that a *Drosophila* strain, *fliA*$^{4}$, mutant in *α-actinin* (Roulier et al., 1992), contains a second mutation that degrades rhabdomere morphogenesis (R. L. Longley, PhD Thesis, Purdue University, 1994). Mutant rhabdomeres are fragmented and inappropriate adhesions join rhabdomeres to rhabdomeres and to stalks of other photoreceptors (Fig. 1B). In occasional planes, all rhabdomeres meet at the ommatidial center, resembling the closed rhabdoms common to most arthropods. We consequently name the gene *eyes closed* (*eyc*). It is notable that the external morphology of *eyc*$^{1}$ eyes is completely normal (data not shown).

*eyc*$^{1}$ photoreceptors are indistinguishable from wild type at 37% p.d.. At this stage, R cell apical membranes contact each other in stereotyped combinations. R2, R4 and R7 contact 'in front of' R3, pre-figuring the trapezoid of the adult ommatidium (Fig. 1E,F). The z.a. junctions that join adjacent R cells appear normal. The apical membranes of wild type and mutant R cells are infolded, but do not show regional differentiation.

By 55% p.d., the *eyc*$^{1}$ phenotype is plain. The IRS fails to open and R cells contact each other in rhabdomere tip-to-tip and rhabdomere-to-stalk contacts (Fig. 1H). Distinctive stalk and rhabdomere membranes are evident, but they are not organized in a simple center-surround. Islands of trapped stalk make loops in R cell cross-sections. Contacts between R cells

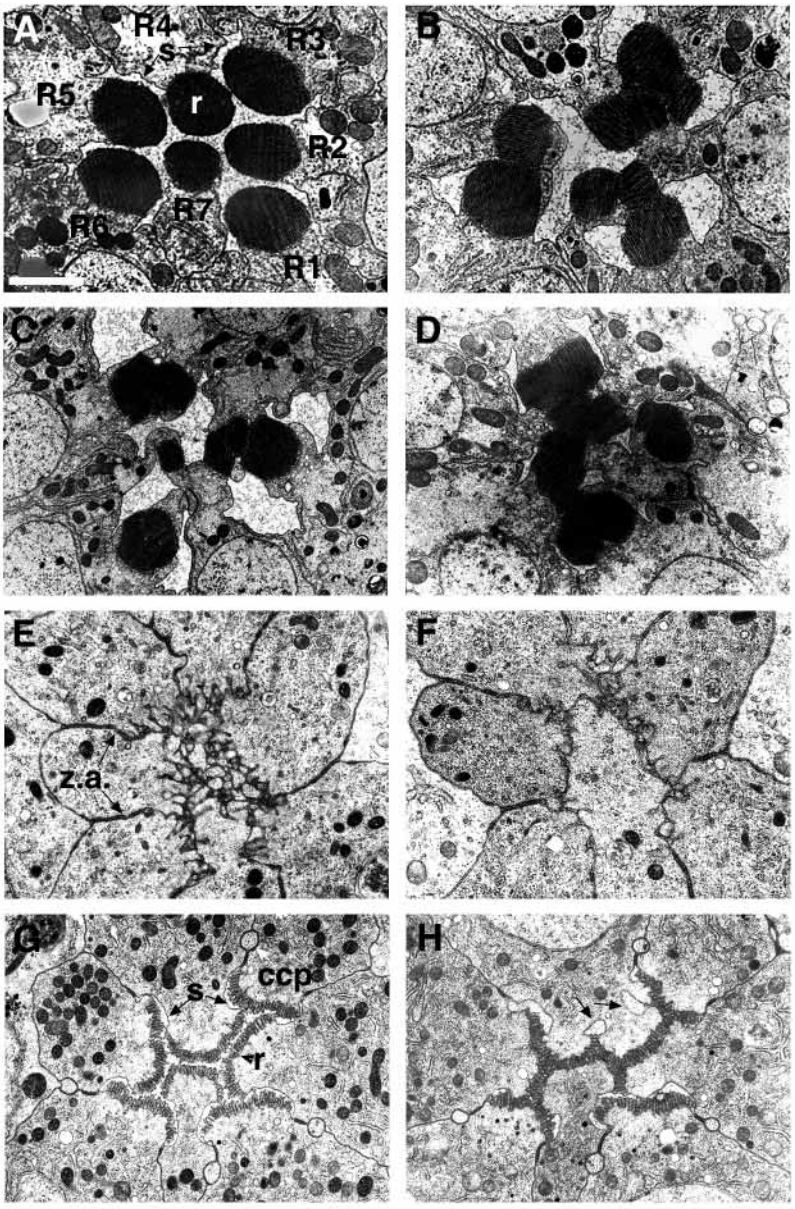


**Fig. 1.** *eyc* is required for normal *Drosophila* photoreceptor morphogenesis. (A) In wild-type eyes, the closely packed photosensitive microvilli of the rhabdomere (r) appear as dark circular ovals arranged in a trapezoid. Rhabdomeres are positioned in the inter-rhabdomeral space (IRS) by a surrounding membrane domain, the stalk (s). Together, the rhabdomere and stalk constitute the photoreceptor apical plasma membrane. (B) In $eyc^1$ eyes, abnormal apical membrane contacts, including rhabdomere-rhabdomere and rhabdomere-stalk contacts, disrupt the rhabdomere trapezoid and partition the IRS into irregular chambers. (C) $eyc^P$ and (D) $eyc^P$ in *trans* with *Df(2R)Px2* show similar disturbances of rhabdomere topology. (E,F) In 37% p.d. wild-type (E) and $eyc^1$ (F) ommatidia, irregularly infolded photoreceptor apical surfaces, which are bounded by zonula adherens (z.a.) junctions, face each other in a trapped apical cavity. (G) By 55% p.d., wild-type photoreceptor apical surfaces have differentiated well-ordered stalk and rhabdomere subdomains. Face to face contacts have been released and the IRS has opened. Processes of the four cone cells (ccp) appear as small circular profiles 'behind' z.a. junctions between photoreceptors. (H) In 55% p.d. $eyc^1$ ommatidia, distinct rhabdomere and stalk membrane can be recognized, but these are irregularly ordered. Face to face apical contacts have not released and the IRS is fragmented into small chambers. Loops of stalk membrane (arrows) are trapped by abnormal adhesions. Scale bar: 2 μm. Anterior is towards the right.

in adult ommatidia commonly include those seen during rhabdomere extension, notably R2/R4/R7; the rhabdomere of R4 frequently bifurcates to contact R2 and R7. Strong R5/R6 contact, not seen between rhabdomeres during extension, is also common in the mutant.

In order to test the hypothesis that persistent contacts between mutant rhabdomeres are due to the inability of R cells to clear adhesive proteins from their apical faces, we examined mutant eyes using phalloidin, anti-Arm, anti-DE-Cad and anti-Crb antibodies. Confocal micrographs of $eyc^1$ 50% p.d. eyes show abnormal Arm staining in R cell apical membranes, often in patches localized to abnormal R cell contacts (Fig. 2A) (*eyc* 50% p.d.). DE-Cad staining is similarly localized to abnormal contacts (Fig. 2B). We speculate that $eyc^1$ R cells are unable to reorganize their apical membranes correctly at this crucial stage of morphogenesis.

Despite the severity of the rhabdomere phenotype, $eyc^1$ eyes show the expression of rhodopsin in outer photoreceptors at the appropriate developmental stage; there is no obvious morphological phenotype beyond rhabdomere malformation (data not shown).

## Eyc encodes a *Drosophila* p47 homolog

Cloning of the *eyc* gene was initiated from an *eyc* P-element allele (P1363), which failed to complement $eyc^1$ (see Materials and Methods). Plasmid rescue of P1363, recovered ~16 kb genomic DNA flanking the P-element. A ~2 kb genomic probe (P3), 3′ to the P-insertion site revealed a ~1.1 kb transcript which is elevated in $eyc^1$ and P1363/*Df(2R) Px2* flies relative to wild type at ~30% p.d. (Fig. 3A). Eyc protein levels are likewise elevated relative to wild type at this stage (Fig. 3B). P3 was then used to screen a *Drosophila* adult head cDNA library and identified a single class of cDNA clone, representing a transcript of 1.1 kb. This 1112 bp cDNA was sequenced on both strands to obtain the gene sequence. Genomic sequence of a P1 clone (DS02336) indicates *eyc* is intronless.

Conceptual translation of the longest ORF predicts a 353 amino acid protein with 46% similarity and 31% identity extending over the entire protein to rat p47, a co-factor that regulates the activity of the AAA ATPase (Patel and Latterich, 1998), p97. Two additional p47 homologs, human p47 and yeast SHP1 have been reported. A ClustalW multiple sequence alignment of the p47 family is shown in Fig. 3D. In addition to *eyc*, the *Drosophila* Genome Project genome predicts a potential p47 homolog, CG11139, localized to 43C4-5; no mutant phenotype or characterization of this gene has been reported.

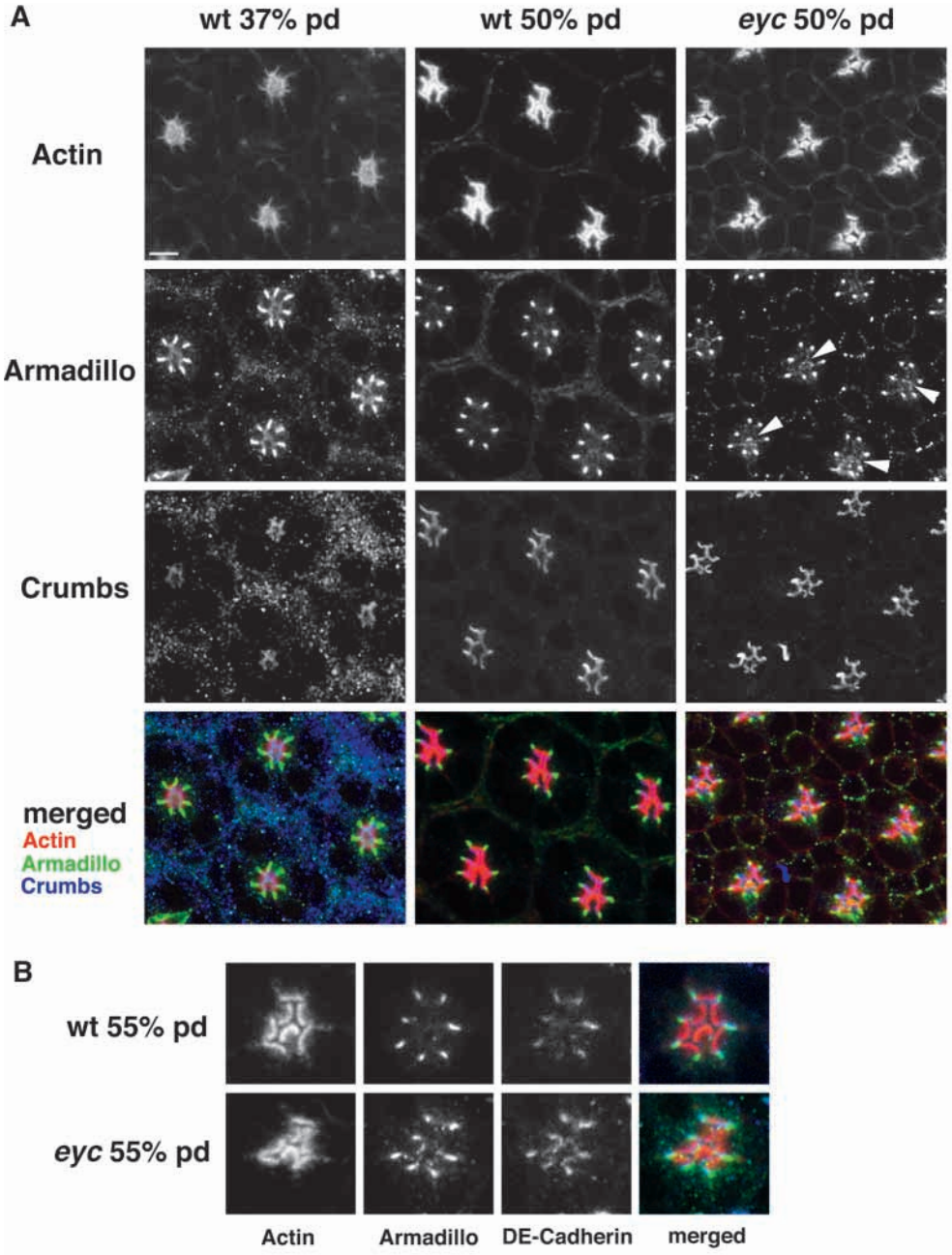


**Fig. 2.** *eyc*$^{1}$ R cells inappropriately retain apical adhesions of rhabdomere extension. (A, left) In 37% p.d. wild-type ommatidia, actin-rich R cell apices face each other in a trapped pocket. Bright 'bars' of Armadillo staining highlight zonula adherens (z.a.) junctions delimiting R cell apical surfaces. At lesser intensity, Armadillo is detected across the entire apical membrane. Crumbs, an apical membrane protein (Tepass, 1996), is also distributed across R cell apical membranes. R cell apices are relatively small at this stage; the trapped apical pocket is approximately 5 μm deep. By 50% p.d. (A, center), definitive, actin-rich rhabdomere primordia are established and have extended to the retinal floor, a depth of approximately 15 μm. The stereotyped pattern of contacts prefiguring the adult trapezoid is evident along the planes of separation opening the IRS. Armadillo has largely retreated to the z.a. junctions. Light apical face staining is often encountered in R7. Crumbs remains across the entire apical surface. (A, right) In 50% p.d. *eyc*$^{1}$ eyes, inappropriate contacts between R cells are evident. Contacts between photoreceptors R2, R4 and R7 are prominent. R5 and R6 often establish strong face to face contact. Arm staining typically marks adhesions (arrowheads). Crumbs staining is normal in the mutant at this stage. (The more open mesh of the pigment cells results from removal of the cornea during dissection.). (B, top) In 55% p.d. wild-type eyes, DE- Cadherin and Armadillo are largely absent from R cell apical surfaces. (bottom) In 55% p.d. *eyc*$^{1}$ ommatidia, bars of colocalized Armadillo and DE-cadherin mark sites of contact. Anterior is towards the right, polar is towards the top. Scale bar: 4 μm.

The site of P-element insertion in P1363 was found 139 bp downstream of the *eyc* gene stop codon (Fig. 3C). In addition, the P-element also carried a 137 bp DNA fragment from 44D1-D2 placed proximal to *eyc*; a fragment of undetermined size is located on the other side of P-element. This suggests the original P1363 strain may contain a deletion resulting from a previous imprecise excision and could account for its homozygous lethality. Recombination of P1363 onto a wild-type second chromosome generated a homozygous viable P1363, *eyc*$^{P}$. *eyc*$^{P}$ ommatidia show the *eyc*$^{1}$ eye phenotype (Fig. 1C). Additionally, this strain shows mild fusion of abdominal tergites.

*eyc* genomic DNA was examined to determine mutant molecular defects. Three independent clones sequenced on both strands showed no alterations in the *eyc* ORF. Two point mutations, an A to G transition 162 bp downstream of the stop codon and a single base deletion 486 bp downstream of the stop codon, were found in *eyc* genomic DNA (Fig. 3C). Since the parental chromosome exposed to ethylmethane sulphate (EMS) mutagenesis is no longer available, it cannot be ruled out these changes are polymorphisms. Nevertheless, the location of these changes and the site of P1363 insertion suggest the observed misexpression of *eyc* may be due to changes in 3′ regulatory elements, as observed for other genes (Zhou et al., 1999).

That *eyc*$^{1}$ and *eyc*$^{P}$ are recessive appears at odds with a hypothesis suggesting transcript elevation causes the eye phenotype: should they not be dominant? Regulation of transcription by interallelic interactions, known in *Drosophila* and elsewhere (Lewis, 1954; Henikoff, 1997), could account

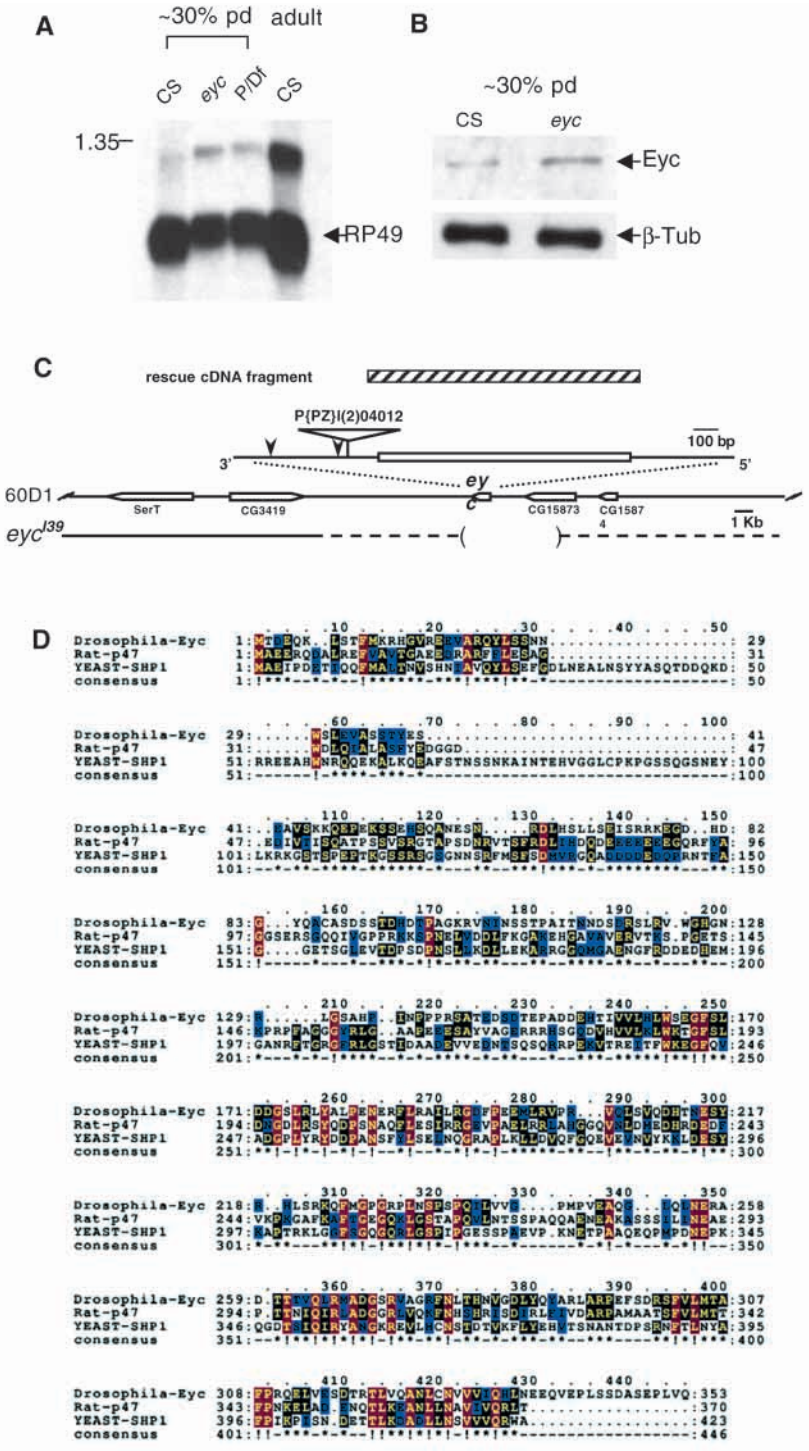


**Fig. 3.** *eyc* encodes a *Drosophila* p47 homolog and *eyc* is misexpressed in early pupae. (A) A Northern blot shows a 2 kb genomic probe detects a 1.1 kb mRNA, the levels of which are elevated at ~30% *eyc* and P1363/*Df(2R)Px2* (P/Df) flies relative to wild type (CS); RP49 was used as loading control. (B) A Western blot shows the anti-Eyc antiserum detects Eyc protein, which is more abundant in ~30% p.d. $eyc^1$ retinal extract compared with wild type at the same developmental stage; β-Tubulin was used as loading control. (C) Molecular map of *eyc* locus. 60D1 represents genome project predicted genomic map of *eyc* locus; predicted genes nearby *eyc* are denoted as white bars with pointed ends indicating transcript orientation. The *eyc* locus is shown above, with the white bar indicating the ORF. The *eyc* allele has two 3′ point mutations (arrowheads). The P-element insertion site of $eyc^P$ allele is shown. The *eyc* null allele $eyc^{l39}$ is shown below 60D1; brackets mark the determined deletion and broken lines indicate undetermined potential deletion. The DNA fragment used to construct the pUAS-eyc transgene is shown as a hatched bar. (D) ClustalW alignment of the predicted Eyc amino acid sequence with two related proteins, rat p47 (human p47 sequence is 95% identical) and yeast SHP1. Residues identical in all three species are shown on a red background and are indicated by '!'; residues identical or with conserved substitutions in two species are shown on black or blue, respectively, and are indicated by an asterisk. The p47/Eyc family shares about 30% protein sequence identity and ~45% similarity. *eyes closed* sequence data are available from GenBank/EMBL/DDBJ under Accession Number AF170565.

for our current observations (Table 1). We consider the possibility that a 3′ suppressor sensitive to epigenetic influences contributes to *eyc* regulation. Analogous to the *trans* activity of the *yellow* enhancer (Morris et al., 1998), pairing a wild-type homolog with an *eyc* mutant may allow recruitment of a suppressor that downregulates transcription of both copies, over-riding decreased binding of a repressive factor by 3′ changes in $eyc^1$ and $eyc^P$. Further genetic and molecular analysis of *eyc* will be required to explore this possibility.

## Temporal misexpression of Eyc produces an eyc-like phenotype

As the temporal misexpression of *eyc* coincides with the developmental stage at which the rhabdomere/stalk organization of the photoreceptor apical surface is established, we hypothesized that Eyc misexpression at this stage might produce an *eyc*-like eye phenotype. In order to test this, we used the GAL4/UAS system (Brand and Perrimon, 1993) to drive Eyc expression at mid-pupal stages and examined its effect on rhabdomere development.

Developmentally staged pupae carrying one copy of *UAS-eyc* and one copy of *Hs-GAL4* were given six cycles of 45 minutes 37°C heat shock and 5 hours 15 minutes 25°C recovery, starting at 30% p.d. Eyes were dissected from freshly eclosed adults and examined using confocal and electron microscopy. We found *eyc*-like defects in the eyes of heat-

**Table 1. *eyc* eye phenotype in different *eyc* alleles and complementation genotypes**

| Genotypes | *eyc* phenotype |
|---|---|
| $eyc^1/eyc^1$ | Yes |
| $eyc^P/eyc^P$ | Yes |
| $eyc^1/eyc^P$ | Yes |
| $eyc^1$/*Df(2R)Px2* | Yes |
| $eyc^P$/*Df(2R)Px2* | Yes |
| $eyc^1$/+ | No |
| $eyc^P$/+ | No |
| *Df(2R)Px2*/+ | No |

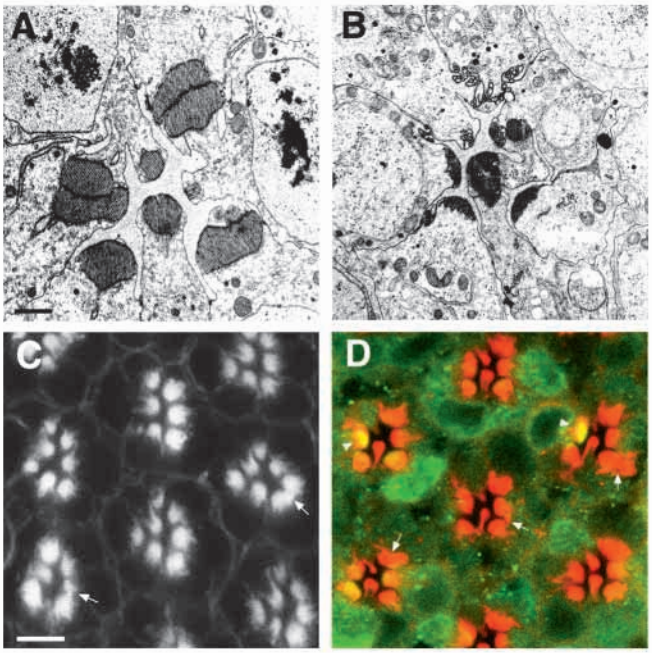


**Fig. 4.** Expression of Eyc in pupae produces an *eyc*-like eye phenotype. (A) Electron micrograph of an adult eye of a *Hs-GAL4/UAS-eyc* fly exposed to six pulses of 45 minutes heat shock starting at 30% p.d. Approximately 23% of ommatidia in which Eyc was transgenically misexpressed show abnormal contact between rhabdomeres. (B) Heat shocks from 30% to 100% p.d. resulted in reduced rhabdomeres with abnormal contacts. Unshocked animals or parallel heat shocks to control flies did not produce rhabdomere defects. (C) Confocal micrographs of phalloidin-stained *GMR-GAL4/UAS-eyc* eyes show abnormal contacts of rhabdomeres (arrows). (D) Confocal micrograph of an *Hs-GAL4/UAS-eyc* eye whole-mount double-labeled with rhodamine-phalloidin (red) and 4C5 anti-Rh1 antibody (green). This animal received the same heat shock regimen as that in B. It shows abnormal rhabdomere adhesion in some photoreceptors (arrows). Deficient delivery of rhodopsin to the rhabdomere is also evident. Arrowheads indicate normal rhodopsin localization in some photoreceptors. *Hs-GAL4* flies that received the same heat shock treatment do not show an eye phenotype. Scale bars: in A, 1 μm in A,B; in C, 5 μm in C,D.

shocked *Hs-GAL4/UAS-eyc* flies (Fig. 4A). In the EM, approximately 23% (21/89) of ommatidia showed abnormal contacts between rhabdomeres. Eyc misexpression started later in pupal development did not generate an *eyc* eye phenotype (data not shown). These results support the hypothesis that the *eyc* phenotype is due to mid-pupal Eyc misexpression.

More severe defects were observed when heat shocks were continued into later pupal stages; rhabdomeres displayed abnormal adhesions and their size was reduced in almost all R cells (Fig. 4B). Moreover, anti-Rh1 immunostaining using 4C5 showed these animals were also deficient in rhodopsin delivery to outer R cell rhabdomeres. Most contained little or no rhodopsin; instead, rhodopsin was concentrated in the photoreceptor cytoplasm (Fig. 4D). Control *Hs-GAL4* flies given the same heat shock regimen did not show a phenotype. *UAS-eyc* driven by *GMR-GAL4*, which induces eyc transgene expression starting immediately behind the furrow in third instar larvae, also generated an *eyc*-like phenotype (Fig. 4C).

## Eyc overexpression results in endoplasmic reticulum expansion

p97 has been shown essential for the budding of vesicles from transitional ER (Zhang et al., 1994) and we explored the possibility that rhodopsin accumulation in the photoreceptor cytoplasm was related to ER defects. We made parallel

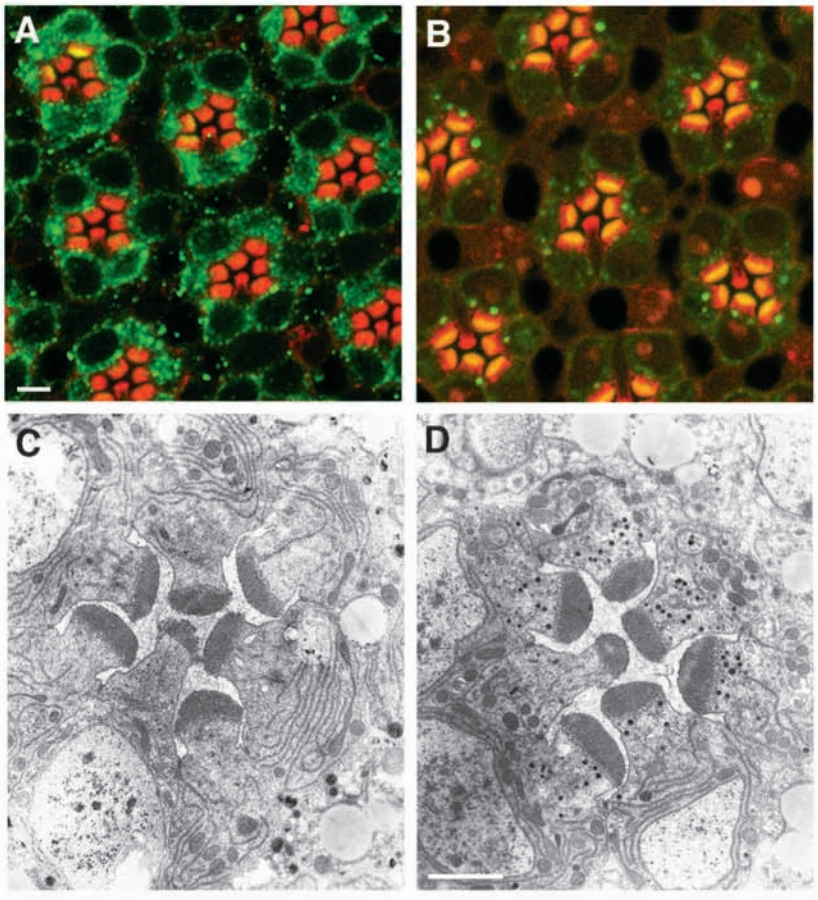


**Fig. 5.** Eyc misexpression increases R cell ER and inhibits rhodopsin delivery to the rhabdomere. In parallel confocal (A,B) and electron microscope (C,D) preparations, *Hs-GAL4/UAS-eyc* flies (A,C) and *Hs-GAL4/+* (B,D) were given three pulses of 1 hour 37°C heat shock with 5 hours 25°C recovery starting at ~70% p.d. After the last recovery, animals were dissected and processed for parallel experimental preparations. For confocal microscopy, retinal whole-mounts were stained using rhodamine-phalloidin (red) and 4C5 anti-Rh1 antibody (green). (A) Eyc overexpression results in rhodopsin accumulation in the cytoplasm and diminished delivery to the rhabdomere. (B) Rhodopsin localization is normal in heat-shocked controls; the central R7 rhabdomere does not express Rh1 and consequently only stains with phalloidin. (C) ER accumulates in photoreceptors overexpressing Eyc. (D) ER is normal in parallel heat-shocked *Hs-GAL4/+* controls. Scale bars: in A, 5 μm in A,B; in D, 2 μm in C,D.

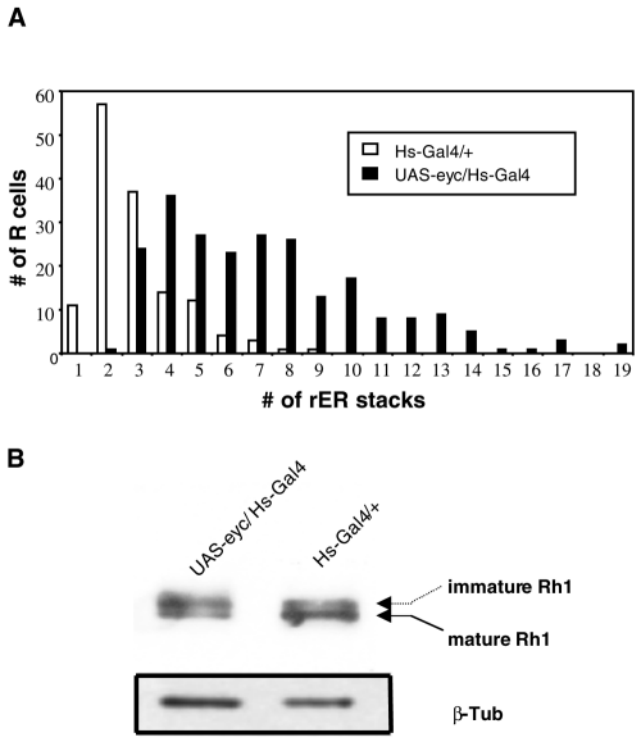


**Fig. 6.** Eyc overexpression causes ER proliferation and inhibition of Rh1 maturation. Quantitation of ER stacks in R cells from the experiment shown in Fig. 5C,D. (A) In *Hs-GAL4/+* control, the majority of R cells show two to three ER stacks per cross section, while heat shocked *Hs-GAL4/UAS-eyc* R cells typically show greater numbers of stacks. (B) Western blot from the parallel experiment shows the overexpression of Eyc inhibits Rh1 maturation. Protein samples were extracted from two eyes; β-Tubulin was used as a loading control. 4C5 anti-Rh1 antibody detects a 35 kDa mature form of Rh1, levels of which are significantly reduced in *Hs-GAL4/UAS-eyc* fly eyes compared with *Hs-GAL4/+*. Additionally, higher molecular weight, immature Rh1 is more abundant in *Hs-GAL4/UAS-eyc* eyes than in the *Hs-GAL4/+* control.

preparations for both anti-Rh1 immunostaining (Fig. 5A,B) and electron microscopy (Fig. 5C,D). *Hs-GAL4/UAS-eyc* animals received three 1 hour heat shocks separated by 5 hours recovery starting at 70% p.d.; eyes were dissected and prepared for observation at approximately 85% p.d. In accordance with results obtained with earlier heat shocks (Fig. 4D), overexpression of Eyc inhibits Rh1 transport to the rhabdomere (Fig. 5A,B). Using electron microscopy, we found abundant ER accumulation in photoreceptor cytoplasm, which is a not seen in control animals (Fig. 5C,D).

In order to quantitate this difference, we collected tangential sections approximately 25 μm below the corneal surface and photographed approximately 20 ommatidia. ER stacks in R cells were counted manually on prints. In *Hs-GAL4/+* controls, the majority of R cells had two to three ER stacks, similar to normal photoreceptors at this stage (data not shown). In *Hs-GAL4/UAS-eyc* flies, R cells showed more ER stacks, ranged from three to 10 stacks (Fig. 6A). We speculate that the cytoplasmic rhodopsin staining observed in the confocal microscope results from disruption of vesicle traffic to the rhabdomere, possibly owing to rhodopsin becoming trapped in the ER.

## Eyc overexpression inhibits rhodopsin delivery

We investigated the impact of Eyc overexpression on rhodopsin synthesis and maturation. In normal photoreceptors, rhodopsin synthesis and core glycosylation in the ER yields immature forms that are deglycosylated in the Golgi before transport of the mature 35 kDa form to the rhabdomere (Colley et al., 1995). If Eyc overexpression disrupts vesicle-mediated protein trafficking, we might expect an increase in immature rhodopsin in *Hs-GAL4/UAS-eyc* eyes. To test this, we heat shocked pupae as before assessed rhodopsin maturation using western blots. Mature rhodopsin levels were decreased in *Hs-GAL4/UAS-eyc* retinas relative to *Hs-GAL4* controls (Fig. 6B), consistent with the reduced stain in rhabdomeres observed using immunohistochemistry. Immature, higher molecular weight rhodopsin was also increased relative to mature rhodopsin in these eyes, suggestive of defects in rhodopsin processing, potentially arising from disturbance of intracellular membrane traffic.

## *eyc* loss-of-function mutations disrupt nuclear envelope assembly

In order to further define the function of Eyc, we used imprecise excision of P1363 to generate loss-of-function *eyc* alleles. We screened 250 lines and recovered 27 homozygous lethal excisions. Embryo development was observed in progeny of 10 balanced excision heterozygotes. In all 10 lines, approximately one quarter of the embryos, later confirmed as lacking the *eyc* ORF using PCR, arrested before cellularization. Three of the lines ($eyc^{l20}$, $eyc^{l27}$ and $eyc^{l39}$) were selected for molecular characterization and rescue experiments (below).

As p97 is sensitive to alkylation by *N*-ethyl-maleimide (NEM), and as in vitro reassembly of *Xenopus* nuclear membrane is NEM sensitive (Macaulay and Forbes, 1996; Marshall and Wilson, 1997), we speculated that p47/Eyc might be essential for nuclear envelope fusion. We stained embryos of $eyc^{l39}/CyO$ inter se crosses with an antibody to Lamin, a nuclear envelope protein that has been shown to play an essential role in nuclear envelope assembly (Burke and Gerace, 1986; Dabauvalle et al., 1991; LenzBohme et al., 1997; Lourim and Krohne, 1993; Chaudhary and Courvalin, 1993; Moir et al., 2000; Newport et al., 1990).

During the first half hour after egg deposition, we observed no differences in the nuclear envelopes of embryos from wild-type or $eyc^{l39}/CyO$ crosses, suggesting early nuclear division in *eyc* nulls proceeds normally using maternally supplied Eyc (data not shown). At 1.5 to 2 hours, wild-type embryos stained with anti-Lamin show two staining patterns: Lamin is either concentrated around the separated M-phase chromosomes (Fig. 7A), consistent with an association between Lamin and chromatin (Moir et al., 2000), or the interphase nuclear envelope is highlighted (Fig. 7B). In $eyc^{l39}/CyO$-derived progeny, approximately one quarter of the embryos show no nuclear envelopes at the same stage (Fig. 7C); occasional embryos showed Lamin aggregates (Fig. 7D), which may be similar to the annulate lamellae observed in *Drosophila lamin* $Dm_0$ (LenzBohme et al., 1997).

Concomitant with loss of the nuclear envelope, the normally dense nuclear DNA seen in zygotic nuclei becomes irregularly fragmented and dispersed. It seems likely that absence of the nuclear envelope results in abnormal chromosome segregation. Probably as a result of destructive mitosis and chromosome dispersal, *eyc* null nuclei do not migrate to the surface of the

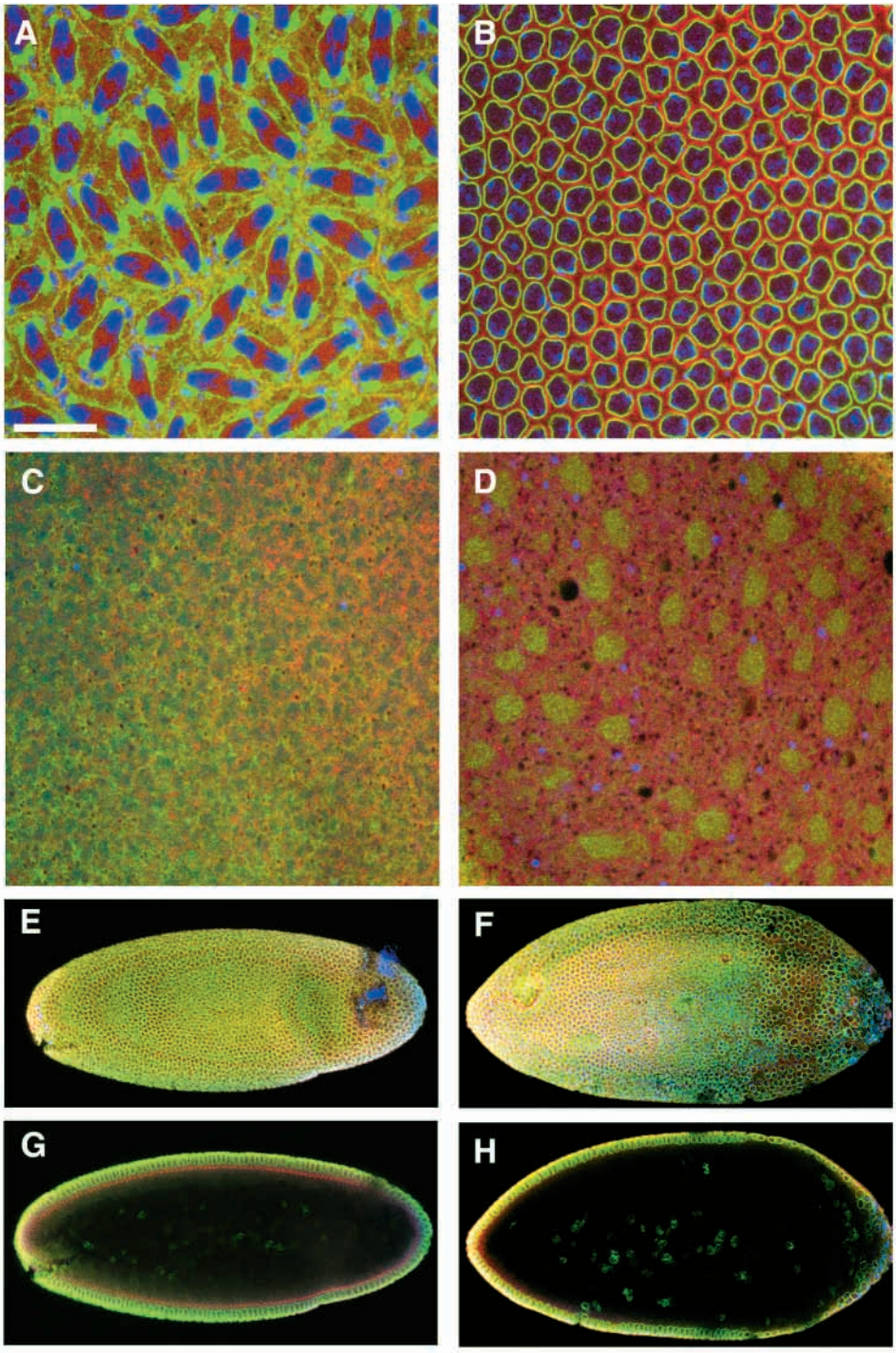


**Fig. 7.** Inhibition of p47/Eyc disrupts nuclear envelope assembly. Wild-type, *eyc*$^{l39}$ (1.5-2 hours at 25°C), and microinjected syncytial blastoderm embryos triple labeled with phalloidin (red), anti-Lamin (green) and YOYO-1 (blue). Confocal images focus on the cortex of the syncytial blastoderm. (A) In wild-type M phase embryos, Lamin staining shows disassembled nuclear envelope while nuclear vesicles congregate the separated chromosomes. (B) Interphase embryos show Lamin staining of nuclear envelopes and a normal hexagonal array of phalloidin staining. Two examples of *eyc*$^{l39}$ embryos show abnormal Lamin staining pattern. (C) A commonly observed *eyc*$^{l39}$ phenotype shows loss of normal staining pattern for the three markers. (D) An optical section of a mutant embryo in the same focal plane as in B shows a cloudy Lamin staining, possibly owing to the aggregation of Lamin-coated nuclear vesicles. (E-H) Microinjection of wild-type stage 2-3 syncytial blastoderm embryos with pre-immune serum (E,G) or anti-Eyc antiserum (F,H). Equal volumes of serum were microinjected at the posterior (right) end of the embryo. (E,F) Projection views of nine sections, 4 μm apart from the cortex to the embryo core. (E) Embryos injected with pre-immune serum show a normal hexagonal array of cortical nuclei (the blue patch at the posterior is a YOYO-1 crystal). (F) Anti-Eyc antiserum-injected embryo shows fewer nuclei in the posterior region with abnormal nuclear aggregates. (G) An optical section through the embryo shows normal, densely-packed cortical nuclei surrounding embryo in a pre-immune serum injected embryo. (H) A corresponding side view of an embryo injected posteriorly with anti-Eyc shows loosely-distributed, spherical nuclei at the posterior. Scale bar: 20 μm in A-D; 100 μm in E-H.

embryo and organize the normal hexagonal actomyosin staining pattern at the embryo membrane; cellularization fails in mutant embryos (Fig. 7C).

### Injection of anti-Eyc antiserum in syncytial blastoderm embryos disrupts cell cycle progression

To further examine Eyc loss-of-function phenotypes, we microinjected anti-Eyc antiserum into the posterior of stage 2-3 embryos and observed its effects on nuclear division using confocal microscopy 1 hour after injection (~ stage 4-5). We found a gradient of cortical nuclear organization across injected embryos: nuclei were dense and regularly arrayed at anterior ends; nuclei were sparse and poorly organized at the posterior (Fig. 7F). Occasional clustered nuclei could be found in the affected region. Control embryos injected with an equal volume of pre-immune serum did not show nuclear disarray (Fig. 7E).

Side views reveal disruption of cellularization in the posterior of anti-Eyc injected embryos. In normal stage 4-5 embryos, and in embryos injected with pre-immune serum, syncytial nuclei are closely packed and cylindrical (Fig. 7G). By contrast, the posterior region of anti-Eyc injected embryos show fewer nuclei

with a spherical shape, presumably a more relaxed shape in the less crowded environment (Fig. 7H). We speculate that the nuclear divisions are slowed in the Eyc-inhibited cytoplasm, perhaps by delays of postmitotic nuclear envelope reassembly.

### Eyc is required for cell viability

Our results shown above indicate Eyc is fundamental to cell cycle progression during embryogenesis. To determine whether Eyc is generally used at different developmental stages and tissues, we applied the EGUF/hid method (Stowers and Schwarz, 1999) to generate homozygous *eyc* null eyes. Eyes are absent in flies in which $eyc^{l39}$ is homozygosed early in the development of the eye primordium (data not shown), supporting a cell-essential role for Eyc.

A cell-essential role for p47/p97 is also suggested by our failure to obtain *ter94* (a *Drosophila* p97 homolog) null eye clones (data not shown), as well as the failure to obtain *ter94* loss-of-function germline clones (Leon and McKearin, 1999).

### An eyc transgene rescues *eyc* lethality

In order to define the deletion resulting from imprecise excision, we synthesized primers to test the integrity of genes neighboring *eyc*. One *eyc* null allele ($eyc^{l39}$) contained a complete downstream neighbor, CG3419, and deleted an upstream gene, CG15873, a predicted endopeptidase and possible additional undefined upstream sequence.

To determine if embryonic lethality was due to the loss of *eyc*, rather than CG15873 or additional upstream genes, we crossed a *UAS-eyc* transgene and an *Hs-GAL4* driver into three different homozygous lethal lines, $eyc^{l20}$, $eyc^{l27}$ and $eyc^{l39}$ ($eyc^{l}$), to generate *UAS-eyc; $eyc^{l}$/SM1; Hs-GAL4/+* lines. The transgene rescued the lethality of all three lines. PCR confirmed the rescued flies lacked the endogenous *eyc* gene. Rescue did not require heat shock, suggesting the basal level of *eyc* transgene expression suffices for viability. Indeed, crosses including constitutive actin- or tubulin-GAL4 drivers were lethal. Rescued $eyc^{l}$ homozygous hold their wings at an abnormal, droopy angle and appear less active than wild type.

## DISCUSSION

We have identified and characterized *Drosophila eyc*, a rat p47 homolog. Gain and loss of Eyc function results in developmental phenotypes that share a common focus of membrane biogenesis. The original *eyc* allele, recovered as a second hit in a strain selected as flightless in an EMS screen, is a gain-of-function mutation that results in Eyc misexpression at the time when photoreceptor apical surfaces must reorganize to relinquish the face-to-face contacts that guide rhabdomere extension to the retinal floor and to establish definitive rhabdomere and stalk subdomains. *eyc* mutants fail to release these contacts and to generate the normal center-surround organization of rhabdomere and stalk membrane. Temporal misexpression in the mutant coincides with a stage in which photoreceptor apical surfaces are undifferentiated, consistent with the participation of both stalk and microvillar membrane in adhesions. We speculate that normally directed membrane traffic is necessary for photoreceptor membrane reorganization, including removal of proteins that promote adhesion, such as Armadillo and DE-Cadherin.

A requirement for Eyc in nuclear envelope reassembly adds a novel role for p47. The failure of nuclear envelope reassembly in *eyc* loss-of-function mutants, and the inhibition of nuclear divisions by anti-Eyc antiserum is consistent with observations that pretreatment of nuclear membrane vesicles with NEM, known to inactivate p97, prevents fusion (Macaulay and Forbes, 1996). The continuity of outer nuclear membranes with the ER, where a role for p47/p97 in membrane fusion is well established, offers a plausible basis for a shared fusion mechanism.

One attractive possibility for the proliferation of ER in response to elevated Eyc is suggested by observations in yeast that excess Sec17p, the yeast α-SNAP homolog, inhibits membrane fusion by stabilizing unproductive *cis*-SNARE pairing (Wang et al., 2000). SNAREs nucleate assembly of the COPII coats that mediate ER-Golgi transport (Springer et al., 1999). As transport vesicle budding must endow the vesicle with SNAREs that are competent to mediate fusion, coat assembly may reject fusion-incompetent *cis*-SNARE complexes. Excess Eyc may shift the balance in favor of fusion-incompetent *cis*-SNARE complexes, hindering budding, increasing the size of the ER and disrupting normal rhodopsin traffic.

Alternate scenarios for an effect of Eyc overexpression include diversion of p97 activity from other tasks. For example, p97 also participates in ubiquitin-dependent protein degradation and nuclear transport pathways, and is targeted to these activities by a protein complex, Ufd1/Npl4, which competes with p47 for binding to p97 (Meyer et al., 2000). Excess Eyc might diminish the availability of p97 for these roles. p47/p97 activity in vitro is stoichiometry dependent (Meyer et al., 1998) and it is possible that excess Eyc produces a sub-optimal ratio, which compromises normal membrane fusion in vivo. Excess Eyc may also impact NSF-mediated pathways as α-SNAP and p47 compete for Golgi syntaxin-5 SNARE complexes (Rabouille et al., 1998).

Rhabdomere defects of *eyc* mutants are provocative in light of the report that anti-NSF and anti-α-SNAP antibodies do not inhibit MDCK apical membrane delivery (Ikonen et al., 1995). SNAREs participate in apical membrane transport and presumably require disassembly after fusion (Low et al., 1998). p47/p97 is an attractive candidate to mediate such disassembly.

It is interesting to consider *Drosophila* photoreceptor morphogenesis against the background of Arthropod eye development generally. Higher Dipterans and some Coleopterans are unusual in having ‘open’ rhabdoms in which separate rhabdomeres individually face the IRS. Rhabdomeres of most insects and crustaceans adhere on the central axis to form a multicellular ‘closed’ rhabdom. As in *Drosophila*, closed rhabdoms develop ‘down’ from the distal, corneal surface of the eye to the retinal floor (Eisen and Youssef, 1980; Hafner and Tokarski, 1998). Rhabdomere contacts of closed rhabdoms display diverse and intriguing patterns which may offer clues to the adhesive rules guiding rhabdomere extension (Paulus, 1979). Perhaps an only small change in the ‘machine language’ of photoreceptor development, regulation of targeted membrane delivery, for example, might allow fly rhabdomeres to unstick after extension, opening the IRS.

We are indebted to Dr R. Longley, Jr for use of his unpublished micrographs in Fig. 1E-H. Dr P. Fisher kindly provided anti-Lamin

antisera, Dr U. Tepass provided anti-Crumbs antibody and Dr T. Uemura provided anti-DE-cadherin antibody. We are grateful to Drs B. Burke, P. Fisher, I. Mellman, T. Schwarz and G. Warren for helpful comments. NIH grant EY10306 supported this work.

## REFERENCES

**Acharya**, **U., Jacobs, R., Peters, J. M., Watson, N., Farquhar, M. G. and Malhotra, V.** (1995). The formation of Golgi stacks from vesiculated Golgi membranes requires two distinct fusion events. *Cell* **82**, 895-904.

**Baumann, O. and Walz, B.** (1989). Topography of $Ca^{+2}$-sequestering endoplasmic reticulum in photoreceptors and pigmented Glial-cells in the compound eye of the honeybee drone. *Cell Tissue Res*. **255**, 511-522.

**Block, M. R., Glick, B. S., Wilcox, C. A., Wieland, F. T. and Rothman, J. E.** (1988). Purification of an N-ethylmaleimide-sensitive protein catalyzing vesicular transport. *Proc. Natl. Acad. Sci. USA* **85**, 7852-7856.

**Brand, A. H. and Perrimon, N.** (1993). Targeted gene-expression as a means of altering cell fates and generating dominant phenotypes. *Development* **118**, 401-415.

**Burke, B. and Gerace, L.** (1986). A cell free system to study reassembly of the nuclear envelope at the end of mitosis. *Cell* **44**, 639-652.

**Chang, H. Y. and Ready, D. F.** (2000). Rescue of photoreceptor degeneration in rhodopsin-null *Drosophila* mutants by activated Rac1. *Science* **290**, 1978-1980.

**Chaudhary, N. and Courvalin, J. C.** (1993). Stepwise reassembly of the nuclear envelope at the end of mitosis. *J. Cell Biol.* **122**, 295-306.

**Colley, N. J., Cassill, J. A., Baker, E. K. and Zuker, C. S.** (1995). Defective intracellular transport is the molecular basis of rhodopsin-dependent dominant retinal degeneration. *Proc. Natl. Acad. Sci. USA* **92**, 3070-3074.

**Dabauvalle, M. C., Loos, K., Merkert, H. and Scheer, U.** (1991). Spontaneous assembly of pore complex-containing membranes (‘annulate lamellae’) in *Xenopus* egg extract in the absence of chromatin. *J. Cell Biol.* **112**, 1073-1082.

**Edwardson, J. M.** (1998).Membrane fusion: All done with SNAREpins? *Curr. Biol.* **8**, R390-R393.

**Eisen, J. S. and Youssef, N. N.** (1980). Fine-structural aspects of the developing compound eye of the honey bee, Apis-Mellifera L. *J. Ultrastruct. Res.* **71**, 79-94.

**Guo, W., Sacher, M., Barrowman, J., Ferro-Novick, S. and Novick, P.** (2000). Protein complexes in transport vesicle targeting. *Trends Cell Biol.* **10**, 251-255.

**Hafner, G. S. and Tokarski, T. R.** (1998). Morphogenesis and pattern formation in the retina of the crayfish Procambarus clarkii. *Cell Tissue Res.* **293**, 535-550.

**Henikoff, S.** (1997). Nuclear organization and gene expression: homologous pairing and long-range interactions. *Curr. Opin. Cell Biol.* **9**, 388-395.

**Ikonen, E., Tagaya, M., Ullrich, O., Montecucco, C. and Simons, K.** (1995). Different requirements For NSF, SNAP, and Rab proteins in apical and basolateral transport in MDCK cells. *Cell* **81**, 571-580.

**Kondo, H., Rabouille, C., Newman, R., Levine, T. P., Pappin, D., Freemont, P. and Warren, G.** (1997). p47 is a cofactor for p97-mediated membrane fusion. *Nature* **388**, 75-78.

**Latterich, M., Frohlich, K. U. and Schekman, R.** (1995). Membrane fusion and the cell cycle: Cdc48p participates in the fusion of ER membranes. *Cell* **82**, 885-893.

**LenzBohme, B., Wismar, J., Fuchs, S., Reifegerste, R., Buchner, E., Betz, H. and Schmitt, B.** (1997). Insertional mutation of the *Drosophila* nuclear lamin Dm(0) gene results in defective nuclear envelopes, clustering of nuclear pore complexes, and accumulation of annulate lamellae. *J. Cell Biol.* **137**, 1001-1016.

**Leon, A. and McKearin, D.** (1999). Identification of TER94, an AAA ATPase protein, as a bam-dependent component of the *Drosophila* fusome. *Mol. Biol. Cell* **10**, 3825-3834.

**Lewis, E. B.** (1954). The theory and application of a new method of detecting chromosomal rearrangements in *Drosophila melanogaster*. *Am. Nat.* **88**, 225-239.

**Longley, R. L. and Ready, D. F.** (1995). Integrins and the Development of 3-Dimensional Structure in the *Drosophila* Compound Eye. *Dev. Biol.* **171**, 415-433

**Lourim, D. and Krohne, G.** (1993). Membrane associated lamins in *Xenopus* egg extracts – Identification of two vesicle populations. *J. Cell Biol*. **123**, 501-512.

**Low, S. H., Chapin, S. J., Wimmer, C., Whiteheart, S. W., Komuves, L. G., Mostov, K. E. and Weimbs, T.** (1998). The SNARE machinery is involved in apical plasma membrane trafficking in MDCK cells. *J. Cell Biol.* **141**, 1503-1513.

**Macaulay, C. and Forbes, D. J.** (1996). Assembly of the nuclear pore: Biochemically distinct steps revealed with NEM, GTP γS, and BAPTA. *J. Cell Biol.* **132**, 5-20.

**Marshall, I. C. B. and Wilson, K. L.** (1997). Nuclear envelope assembly after mitosis. *Trends Cell Biol*. **7**, 69-74.

**Mayer, A., Wickner, W. and Haas, A.** (1996). Sec18p (NSF) driven release of sec17p (α-SNAP) can precede docking and fusion of yeast vacuoles. *Cell* **85**, 83-94.

**Mellman, I.** (1995). Enigma variations – protein mediators of membrane fusion. *Cell* **82**, 869-872.

**Mellman, I. and Warren, G.** (2000). The road taken: past and future foundations of membrane traffic. *Cell* **100**, 99-112.

**Meyer, H. H., Kondo, H. and Warren, G.** (1998). The p47 co-factor regulates the ATPase activity of the membrane fusion protein, p97. *FEBS Lett*. **437**, 255-257.

**Meyer, H. H., Shorter, J. G., Seemann, J., Pappin, D. and Warren, G.** (2000). A complex of mammalian Ufd1 and Npl4 links the AAA-ATPase, p97, to ubiquitin and nuclear transport pathways. *EMBO J*. **19**, 2181-2192.

**Moir, R. D., Yoon, M., Khuon, S. and Goldman, R. D.** (2000). Nuclear lamins A and B1: different pathways of assembly during nuclear envelope formation in living cells. *J. Cell Biol.* **151**, 1155-1168.

**Morris, J. R., Chen, J.-L., Geyer, P. K., Wu, C.-T.** (1998). Two modes of transvection: Enhancer action in *trans* and bypass of a chromatin insulor in *cis*. *Proc. Natl. Acad. Sci. USA* **95**, 10740-10745.

**Newport, J. W., Wilson, K. L. and Dunphy, W. G.** (1990). A lamin independent pathway for nuclear envelope assembly. *J. Cell Biol.* **111**, 2247-2259.

**Patel, S. and Latterich, M.** (1998). The AAA team: related ATPases with diverse functions. *Trends Cell Biol*. **8**, 65-71.

**Paulus, H. F.** (1979). Eye structure and the monophyly of the arthropods. In *Arthropod Phylogeny* (ed. A. P. Gupta), pp. 299-383. New York: Van Nostrand Reinhold Company.

**Rabouille, C., Kondo, H., Newman, R., Hui, N., Freemont, P. and Warren, G.** (1998). Syntaxin 5 is a common component of the NSF- and p97-mediated reassembly pathways of Golgi cisternae from mitotic Golgi fragments *in vitro*. *Cell* **92**, 603-610.

**Rabouille, C., Levine, T. P., Peters, J. M. and Warren, G.** (1995). An NSF-like ATPase, p97, and NSF mediate cisternal regrowth from mitotic Golgi fragments. *Cell* **82**, 905-914.

**Rothman, J. E. and Warren, G.** (1994). Implications of the SNARE hypothesis for intracellular membrane topology and dynamics. *Curr. Biol.* **4**, 220-233.

**Roulier, E. M., Fyrberg, C. and Fyrberg, E.** (1992). Perturbations of *Drosophila* α-Actinin cause muscle paralysis, weakness, and atrophy but do not confer obvious nonmuscle phenotypes. *J. Cell Biol.* **116**, 911-922.

**Roy, L., Bergeron, J. J. M., Lavoie, C., Hendriks, R., Gushue, J., Fazel, A., Pelletier, A., Morre, D. J., Subramaniam, V. N., Hong, W. J. et al.** (2000). Role of p97 and syntaxin 5 in the assembly of transitional endoplasmic reticulum. *Mol. Biol. Cell* **11**, 2529-2542.

**Smith, D. E. and Fisher, P. A.** (1989). Interconversion of *Drosophila* nuclear lamin isoforms during oogenesis, early embryogenesis, and upon entry of cultured cells into mitosis. *J. Cell Biol.* **108**, 255-265.

**Spradling, A. C. and Rubin, G. M.** (1982). Transposition of cloned P-elements into *Drosophila* germ line chromosomes. *Science* **218**, 341-347.

**Springer, S., Spang, A. and Schekman, R.** (1999). A primer on vesicle budding. *Cell* **97**, 145-148.

**Stowers, R. S. and Schwarz, T. L.** (1999). A genetic method for generating *Drosophila* eyes composed exclusively of mitotic clones of a single genotype. *Genetics* **152**, 1631-1639.

**Stuurman, N., Maus, N. and Fisher, P. A.** (1995). Interphase phosphorylation of the *Drosophila* nuclear lamin- site mapping using a monoclonal antibody. *J. Cell Sci*. **108**, 3137-3144.

**Tepass, U.** (1996). Crumbs, a component of the apical membrane, is required for zonula adherens formation in primary epithelia of *Drosophila*. *Dev. Biol.* **177**, 217-225.

**Tomlinson, A. and Ready, D. F.** (1987). Neuronal differentiation in the *Drosophila* ommatidium. *Dev. Biol.* **120**, 366-376.

**Uemura, T., Oda, H., Kraut, R., Hayashi, S., Kotaoka, Y. and Takeichi, M.** (1996). Zygotic *Drosophila* E-cadherin expression is required for

processes of dynamic epithelial cell rearrangement in the *Drosophila* embryo. *Genes Dev.* **10**, 659-671

**Wang, L., Ungermann, C. and Wickner, W.** (2000). The docking of primed vacuoles can be reversibly arrested by excess Sec17p (α-SNAP). *J. Biol. Chem.* **275**, 22862-22867.

**White, R. A. H.** (1998). Immunolabelling of *Drosophila*. In *Drosophila, A Practical Approach* (ed. D. B. Roberts), pp. 215-240. Oxford: IRL Press.

**Yamada, T., Okuhara, K., Iwamatsu, A., Seo, H., Ohta, K., Shibata, T. and Murofushi, H.** (2000). p97 ATPase, an ATPase involved in membrane fusion, interacts with DNA unwinding factor (DUF) that functions in DNA replication. *FEBS Lett.* **466**, 287-291.

**Zhang, L., Ashendel, C. L., Becker, G. W. and Morre, D. J.** (1994). Isolation and characterization of the principal ATPase associated with transitional endoplasmic reticulum of rat liver. *J. Cell Biol.* **127**, 1871-1883.

**Zhou, J., Ashe, H., Burks, C., Levine, M.** (1999). Characterization of the transvection mediating region of the *Abdominal-B* locus in *Drosophila*. *Development* **126**, 3057-3065.